Indian Journal of Pure & Applied Physics
Vol. 60, February 2022, pp. 157-162

Acoustic-Phonon Mediated Cyclotron Resonance Power Absorption in Zinc Oxide Free-Standing Nanostructure

Shruti Bhat[a,*], J S Bhat[a] & B G Hegde[b]

[a]Department of Physics, Karnatak University, Dharwad, Karnataka State-580 003, India
[b]Department of Physics, Rani Channamma University, Belagavi, Karnataka State-591 156, India

Received 31 August 2021; accepted 14 January 2022

The phenomenon of cyclotron resonance power absorption when electrons are scattered by acoustic-phonons in ZnO free standing nanostructure (FSNS) is presented. The calculation is based on quantum mechanical perturbation technique. The dependence of power absorption on frequency, magnetic field, temperature and thickness of the FSNS is presented. FWHM or line-width of the resonance power absorption peaks is calculated using profile method and the influence of magnetic field, temperature and thickness of the FSNS is investigated, that the line-width is proportional to magnetic field whereas it is independent of temperature and thickness of FSNS. This theoretical analysis gives insights about magneto-optical properties of FSNS of ZnO which is essential for further experimental investigations.

Keywords: Transparent conducting oxide, Free standing nanostructure, Absorption power, Cyclotron-phonon resonance, Line-width

1 Introduction

In recent years, metal oxide semiconductors have attracted much interest due to their technologically important properties like optical transparency, high electron mobility, wide band gap *etc*, and their application in fabricating variety of devices[1-3]. Metal oxide thin films, with thickness less than carrier mean free path exhibit novel optical and electrical properties[4], catalytic properties[5], due to quantum confinement effects. Thin-film technology is one of the most recent and an active area of research has resulted in the development of new technologies to meet up the requirements of the growing semiconductor industry.

Two-dimensional transparent metal oxide semiconductors, like ZnO thin films, are ideal systems for studying dimensionally confined transport phenomenon study. ZnO has high exciton binding energy of around 60meV and a wide direct band gap of about 3.37eV at room temperature[6]. The band gap of the material can be tuned by an external magnetic field. An external quantized magnetic field **B** perpendicular to the two-dimensional thin film leads to quantization of Landau-levels and broadening of Landau level is due to scattering of carriers. When the material is subjected to both electromagnetic wave and a uniform static magnetic field, cyclotron phonon resonance can be observed with the magneto-optical transition of carriers between Landau energy levels with the simultaneous emission or absorption of phonons and it gives the direct information about effective mass, nonparabolicity of conduction and valence bands and electron-phonon scattering processes[7-9]. At low temperature, electron-acoustic phonon interaction plays dominating role over electron-optical phonon scattering. In the presence of magnetic field, cyclotron-acoustic phonon resonance is the useful tool to understand the electron-acoustic phonon scattering phenomenon. This field has attracted the minds of broad scientific community from theorists[10] to experimentalists[11], because it will provide the information about crystals, novel characteristics and magneto-optical properties of quasi two dimensional electron gas for manufacturing electronic-optoelectronic devices.

Line-width or FWHM of cyclotron phonon resonance power absorption peaks is used as a tool to investigate the transport properties of the material as well as mechanism of electron scattering[11-13]. The cyclotron-resonance line-width is studied for electron-polar optical phonon for different structural systems like quantum wells[14], quantum wire[15], quantum dot[16] and monolayer of the materials[17], but a very few works on this field have been found for electron-

*Corresponding author: (E-mail: shrutibhat165@gmail.com)

acoustic phonon interaction in usual semiconducting materials[18]. So we feel that study of this property in transparent two-dimensional structures is very essential.

Phonon assisted cyclotron resonance is examined in GaAs quantum well structures and cyclotron-acoustic phonon resonance is examined via the magneto-optical power absorption[19,20]. An electron-phonon coupling in graphene for the transverse and longitudinal acoustic phonons has been calculated using first-principles approach[21]. A theoretical study of modification of the energy spectrum of long-wavelength acoustic phonons due to the electron-phonon interaction in a three-dimensional topological Weyl semimetal under the influence of quantizing magnetic fields at low temperatures is done by Song-Bo Zhang and Jianhui Zhou[22]. Electron-phonon scattering is studied within an effective-mass theory in carbon nanotubes[23]. The energy relaxation rate due to phonon scattering of a quasi two-dimensional electron gas is calculated for a GaAs quantum well in the presence of a strong magnetic field[24].

In this article, we obtain the explicit expression for cyclotron-acoustic phonon resonance power absorption(CAPRPA) in the presence of magnetic field and applied to study cyclotron phonon resonance power absorption in FSNS of ZnO when electrons interact with the bulk acoustic phonon modes at low temperature. In section II, a quantum mechanical theory of optical absorption in FSNS subjected to an external magnetic field, applied perpendicular to the plane of FSNS is presented. Calculation of dependence of optical absorption power on frequency and dependence of line-width in terms of FWHM of absorption peaks on magnetic field, temperature and thickness of the material is presented in section-III and depicted the summary and conclusions of this work in last section-IV.

2 Theory

In this study, we consider a FSNS of ZnO applied with a perpendicular static magnetic field $\vec{\mathbf{B}}$. The electrons in the system are free to move in *x*–*y* plane but spatially confined in the *z*-direction. Due to applied magnetic field and spatial confinement in the *z*-direction, electron energy is quantised completely into discrete energy levels as well as Landau levels in *z*- direction.

The one-electron eigenfunctions ψ_{Nlk_y} and energy eigenvalues E_{Nlk_y} are given by[25]

$$\psi_{Nlk_y} = \left(\frac{2}{L_y L_z}\right)^{1/2} \phi_N\left(\frac{x-\lambda^2 k_y}{\lambda}\right)\exp(ik_y y)\sin\left(\frac{l\pi z}{L_z}\right) \quad \ldots (1)$$

$$E_{Nlk_y} = \left(N+\frac{1}{2}\right)\hbar\omega_c + l^2 E_0 \quad \ldots (2)$$

where $E_0 = \frac{\hbar^2\pi^2}{2m^* L_z^{\,2}}$ is the lowest electric subband energy with L_z being the thickness of the FSNS and N = 0,1,2,…. is the Landau level index, l = 1,2,3,…. electric subband index. Also $\omega_c = \frac{|e|B}{m^* c}$ is the cyclotron frequency with e and m^* being the charge and effective mass of the electron, respectively. ϕ_N represents harmonic oscillator wave function and $\lambda = \left(\frac{\hbar}{m^*\omega_c}\right)^{1/2}$ the radius of cyclotron orbit. Expression for absorption power is given by[26]

$$P(\Omega) = \frac{F_0^{\,2}\sqrt{\varepsilon}}{8\pi}\sum_i W_i f_i \quad \ldots (3)$$

where F_0 is the intensity of the incident radiation, ε the dielectric constant and f_i the electron distribution function. The sum is taken over all possible initial states '*i*' of the system. The transition probability, $W_i^{ab(em)}$, due to electron-photon-phonon interaction is given by the second order Fermi's golden rule approximation[27]

$$W_i^{ab,em} = \frac{2\pi}{\hbar}\sum_f \left|\langle f|M|i\rangle\right|^2 \times \delta(E_f - E_i \mp \hbar\omega_q \mp \hbar\Omega) \quad \ldots (4)$$

with E_i and E_f being the initial and final state energies of the electron. $\hbar\Omega$ and $\hbar\omega_q$ represent energies of photon and acoustic phonon, respectively. Matrix element for electron-photon-phonon interaction is

$$\langle f|M|i\rangle = \sum_\alpha\left(\frac{\langle f|H_{rad}|\alpha\rangle\langle\alpha|H_{el-ph}|i\rangle}{E_i - E_\alpha \pm \hbar\omega_q} + \frac{\langle f|H_{el-ph}|\alpha\rangle\langle\alpha|H_{rad}|i\rangle}{E_i - E_\alpha \pm \hbar\Omega}\right) \quad \ldots (5)$$

where H_{rad} is the interaction Hamiltonians with the radiation field and $H_{el\text{-}ph}$ is the interaction Hamiltonians with phonons. The summation is over all the intermediate states α of the present system.

Assuming electromagnetic field is linearly polarized transverse to the magnetic field, the matrix elements for interaction with the photons can be written as

$$\langle N+1|H_{rad}|N\rangle = \frac{e\hbar}{m^*}\left(\frac{2\pi N_v}{\hbar\Omega\varepsilon D}\right)^{1/2}\left(\frac{\hbar m^*\omega_c}{2}\right)^{1/2}\times(N+1)^{1/2}\delta_{N,N+1}\delta_{k_y k_y'}\delta_{ll'} \quad \ldots (6)$$

where N_v the number of photons, Ω the photon frequency and D is the volume of FSNS.

Electron-acoustic phonon matrix element can be written as[12,28]:

$$\langle f|H_{el-ph}|i\rangle = V(q)\left(N_q+\frac{1}{2}\mp\frac{1}{2}\right)^{1/2}F_{ll'}(\pm q_z)J_{NN'}(q_\perp)\delta_{k_y\pm q_y,k_y'} \quad \ldots (7)$$

where ,*V(q)* refers to the strength of electron-acoustic phonon interaction and $\vec{q}=(q_\perp,q_z)$. N_q the Bose distribution function and the overlap integral $F_{ll'}(\pm q_z)$ is given by[28,29]

$$F_{ll'}(\pm q_z) = \frac{2}{L_z}\int_0^{L_z}\sin\left(\frac{l'\pi z}{L_z}\right)\sin\left(\frac{l\pi z}{L_z}\right)\exp(\pm iq_z z)dz \quad \ldots (8)$$

and the Bessel function $J_{NN'}$ is given by[28,29]

$$|J_{NN'}(q_\perp)|^2 = (N!/N'!)\exp\left(-\frac{\lambda^2 q_\perp^{\,2}}{2}\right)\left(\frac{\lambda^2 q_\perp^{\,2}}{2}\right)^{N'-N}\times\left[L_N^{\,N'-N}\left(\frac{\lambda^2 q_\perp^{\,2}}{2}\right)\right]^2 \quad \ldots (9)$$

where $N'>N$, and $L_N^{\,N'-N}$ being the associated Laguerre polynomials.

V(q) in Eq.(8) represents the strength of electron-phonon interaction. For acoustic phonons *V(q)*is given by

$$|V(q)|^2 = \frac{\hbar E_d^{\,2}}{2u\rho V}q \quad \ldots (10)$$

where, E_d denotes the deformation potential constant, u the sound velocity and ρ refers to the mass density of the material.

In order to calculate the absorption power, we may use the approximation for N_q as $N_q+1\approx N_q\approx\frac{k_B T}{\hbar u q}$, with $\omega_q = uq$, so we have

$$\left(N_q+\frac{1}{2}\mp\frac{1}{2}\right)|V(q)|^2 = \frac{k_B T E_d^{\,2}}{2u^2\rho V} \quad \ldots (11)$$

Assuming non-degenerate electron gas in the system, the electron distribution function in the presence of quantizing magnetic field can be written as

$$f_{Nlk_y} = \frac{n_e\pi\lambda^2 L_z}{\gamma}\exp\left(-\frac{E_{Nl}}{k_B T}\right), \quad \ldots (12)$$

$$\text{with } \gamma = \sum_{Nl}\exp\left(-\frac{E_{Nl}}{k_B T}\right) \quad \ldots (13)$$

and n_e refers to the electron concentration.

Using Eq. (11) and performing integrals over q_z and $q_\perp$, we obtain the expression in the extreme quantum limit i.e., when $l=l'=1$

$$P(\Omega,\omega_c,\omega_q) = \frac{3F_0^{\,2}E_d^{\,2}e^2 n_e N_v k_B T}{128m^*\sqrt{\varepsilon}\gamma\hbar u^2\rho L_z\lambda^2}\left\{\frac{1}{(\omega_c-\Omega)^2}+\frac{1}{(\omega_c+\Omega)^2}\right\} \times\sum_N\sum_{N'}\exp\left(-\frac{E_{N1}}{k_B T}\right)(N'+N+1)\left\{\delta\left[\left(N'-N\right)\hbar\omega_c-\hbar\Omega\right]\right\} \quad \ldots (14)$$

where, $E_{N1} = \left(N+\frac{1}{2}\right)\hbar\omega_c + E_0$

Following the collision broadening[29], delta function in Eq. (14) is replaced by Lorentzian of width Γ to get the following expression

$$\delta(M) = \frac{1}{\pi}\frac{\hbar\Gamma}{M^2+\hbar^2\Gamma^2} \quad \ldots (15)$$

where, $M = \left(N'-N\right)\hbar\omega_c-\hbar\Omega$ and Γ is inverse relaxation time for electrons

$$\left(\Gamma^{\mp}\right)^2 = \frac{2\pi}{\hbar}\sum_q\left(N_q+\frac{1}{2}\mp\frac{1}{2}\right)|V(q)|^2\left|F_{ll'}(\pm q_z)\right|^2\left|J_{NN'}(q_\perp)\right|^2 \quad \ldots (16)$$

Numerically we can deduce the significant physical conclusions by taking absorption spectra in section III.

3 Results and Discussion

The numerical results of absorption power obtained in the case of a FSNS of thickness L_z = 5 nm subjected to magnetic field B = 10T and temperature T = 20K

are presented. The material parameters[30-32] used are $m^* = 0.25m_0$, $\varepsilon = 8.1$, $n_e = 8.6\times10^{18}$ cm^{-3}, $E_d = 3.8$eV, $u = 6.59\times10^3$cm/s, $\rho = 6.1$g/cm^3. Fig. 1 shows the variation of absorption power with the Ω/ω_c for acoustic phonons. Absorption spectrum consisting peaks corresponds to the resonant transition of electron between the Landau levels within the first electric sub and $(l = l' = 1)$. These transitions between the Landau levels are due to photon occur at $\Omega = p\omega_c$ (p = 1,2,…), which represents pure cyclotron resonance. The photon energy is absorbed by the electron while simultaneously interacting with acoustic phonon. As a result electron undergoes transition from a lower Landau levels to higher Landau levels spread within first electric subband. The variation of intensity of a selected peak with magnetic field is shown in Fig. 2. The Intensity of the peak is decreases with the increasing photon frequency.

Fig. 3 shows the shift in the position of peak with respect to magnetic field. The transition of electron between Landau levels involves the acoustic phonon scattering, however, involvement of the acoustic phonons is limited to the momentum conservation. Therefore, the absorption spectrum appears like a pure cyclotron resonance.

The influence of the external magnetic field on the FWHM of CAPRPA peaks and intensity of the peaks is significant. The cyclotron radius decreases with increasing magnetic field, leading to increased magnetic confinement. At the same time the Landau level separation also increases leading to reduction in the probability of transition of electrons between the Landau levels if the energy of the Photon is different from the energy separation of the Landau levels. Fig. 4 shows the variation of FWHM with magnetic field. FWHM of CAPRPA peaks increases with increasing magnetic field is due to enhancement in the scattering of electrons. Broadening of the energy levels is studied by calculating line-width in terms of FWHM of the peaks by computation using profile method.

Fig. 5 shows peaks corresponding to $p = 2$, calculated for different temperatures. The position of the peak is not changing with temperature. However, the line-width is slightly increasing with the temperature of the specimen. Though the width of the peaks seems to be increasing on increase in the temperature in the Fig. 5, it is not altering much and remaining almost constant for the temperature range

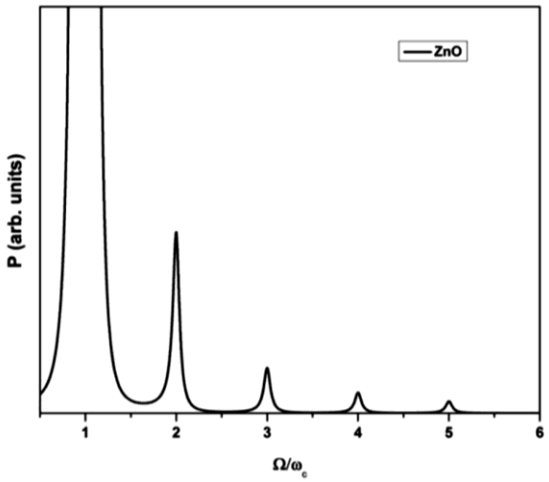

Fig. 1 — Absorption power plotted as a function of Ω/ω_c for FSNS of ZnO of thickness 5nm with an external magnetic field B = 10T and temperature T = 20K.

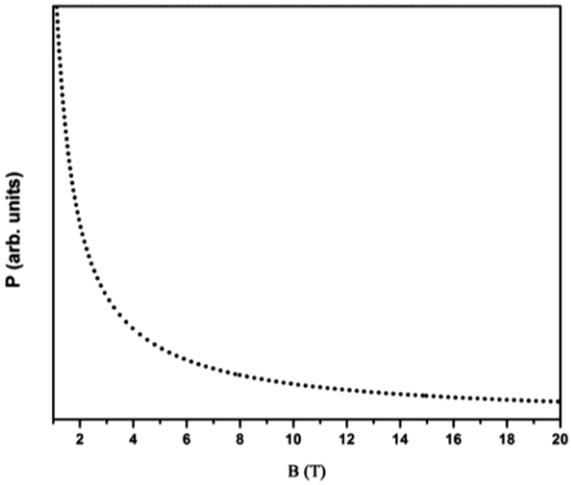

Fig. 2 — Magnetic field dependence of CAPRPA peak values at Ω=3ω_c, calculated for FSNS of ZnO of thickness 5 nm with the temperature T = 20K.

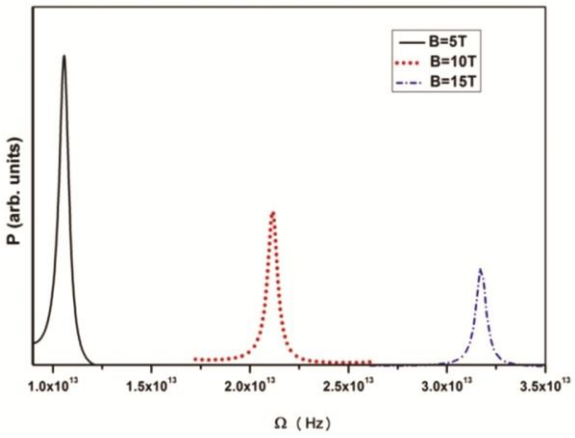

Fig. 3 — Absorption power plotted as a function of Ω for FSNS of ZnO of thickness 5 nm for different magnetic fields at temperature T = 20K.

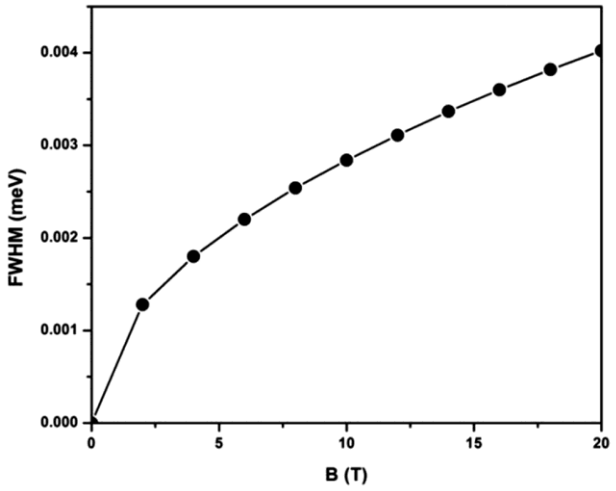

Fig. 4 — FWHM of CAPRPA peaks plotted as a function of magnetic field at T = 20K and L_z = 5 nm.

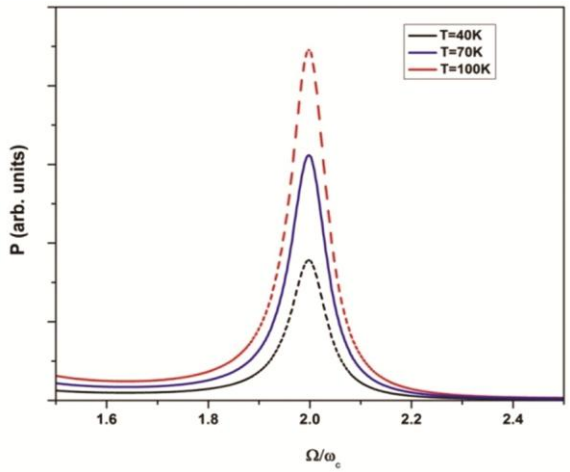

Fig. 5 — Absorption power plotted as a function of Ω/ω_c for FSNS of ZnO of thickness 5nm and magnetic field B=10T for different temperatures.

considered as shown in the Fig. 6. So the FWHM is independent of temperature which is qualitatively consistent with the results obtained for polar optical phonons in graphene[33,34]

Fig. 7 presented to show that the position of the CAPRPA peaks is not affected by the thickness of the material because the resonance condition $\Omega = p\omega_c$ does not depend on the thickness. Also, the FWHM of CAPRPA peaks is independent of the thickness of the material. As we can see in the Fig. 8, FWHM is not changing and nearly constant on increasing the thickness of the FSNS. So, FWHM is independent of both temperature and thickness of the material for electron-acoustic phonon scattering.

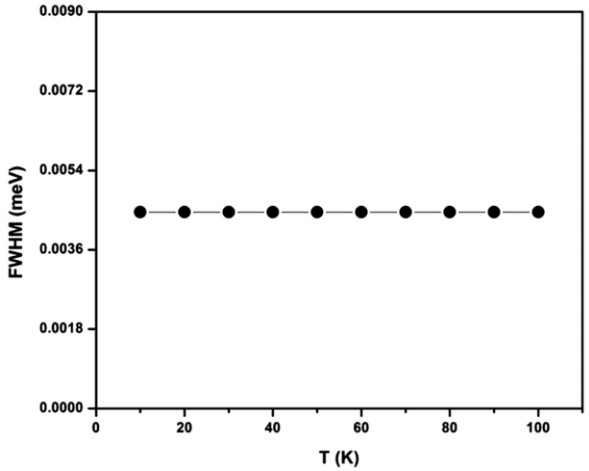

Fig. 6 — FWHM of CAPRPA peaks plotted as a function of temperature at B = 10T and L_z = 5 nm.

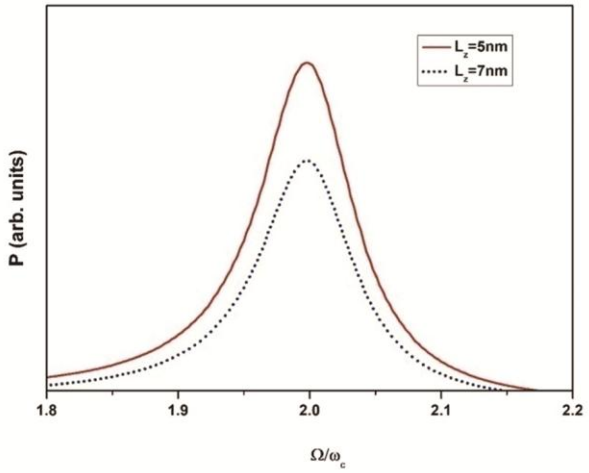

Fig. 7 — Absorption power plotted as a function of Ω/ω_c for FSNS of ZnO, B = 10T and T = 20K for different thickness.

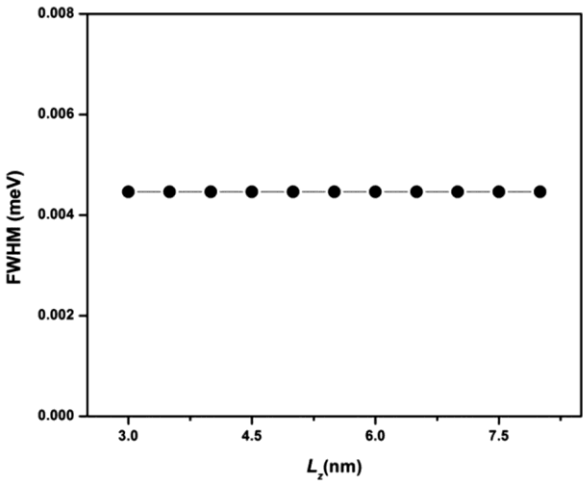

Fig. 8 — FWHM as a function of thickness (L_z) of ZnO FSNS at B = 10T and T = 20K.

4 Conclusion

We have theoretically investigated the intrasubb and electron scattering by acoustic-phonons in free standing nanostructure of ZnO in the presence of a uniform quantizing magnetic field. The expression for absorption power is obtained and the numerical results are presented in graphical form. We find that at low temperatures, electron-acoustic phonon scattering plays an important role in the phenomena of cyclotron phonon resonance. FWHM of CAPRPA peaks increases with the rise of external magnetic field, but it is independent of the temperature and the thickness of the material. The position of CAPRPA peaks is not altered with the temperature and thickness of the material, where as peak positions are shifting considerably with the change in the magnetic field. These results would be helpful to conduct experimental investigation of optical and electronic properties of nano-electronic devices in the future.

Acknowledgment

This work was supported by UGC-SAP-CAS-PHASE-II programme, India.

Appendix

Integral over q_z is calculated

$$\int_{-\infty}^{+\infty} \left|F_{ll'}(q_z)\right|^2 dq_z = \frac{\pi}{L_z}\left(2+\delta_{ll'}\right)$$

Also, the integral of Bessel function with respect to $q_\perp$ is given as follows[20] $\int_0^\infty q_\perp{}^3 \left|J_{NN'}(q_\perp)\right|^2 dq_\perp = \frac{2}{\lambda^4}(N+N+1)$

References

1 Tereshchenko A, Yazdi G R, Konup I, Smyntyna V, Khranovskyy V, Yakimova R & Ramanavicius A, *Colloids Surf B: Biointerfaces*, 191 (2020) 110999.
2 Shi W, Ahmed M M, Li S, Shang Y, Liu R, Guo T, Zhao R, Li J & Du J, *ACS Appl Nano Mater*, 2 (2019) 5430.
3 Kim B H, Staller C M, Cho S H, Heo S, Garrison C E, Kim J & Milliron D J, *ACS Nano*, 12 (2018) 3200.
4 Sarma B & Sarma B K, *J Alloys Compd*, 734 (2018) 210.
5 Enferadi-Kerenkan A, Ello A S & Do T O, *Indus Eng Chem Res*, 56 (2017) 10639.
6 Ellmer K, *J Phys D: Appl Phys*, 34 (2001) 3097.
7 Fang X, Zheng F, Drachenko O, Zhou S, Zheng X, Chen Z, Wang P, Ge W, Shen B, Feng J & Wang X, *Superlatt Microstruct*, 136 (2019) 106318.
8 Xia C Q, Monti M, Boland J L, Herz L M, Lloyd-Hughes J, Filip M R & Johnston M B, *Phys Rev B*, 103 (2021) 245205.
9 Badjou S & Argyres P N, *Phys Rev B*, 35 (1987) 5964.
10 Kang N L & Lee J H & Choi S D, *J Korean Phys Soc*, 37 (2000) 339.
11 Kobori H, Ohyama T & Otsuka E, *J Phys Soc Jpn*, 59 (1990) 2141.
12 Cho Y J & Choi S D, *Phys Rev B*, 49 (1994) 14301.
13 Sug J Y, Jo S G, Kim J, Lee J H & Choi S D, *Phys Rev B*, 64 (2001) 235210.
14 Hien N D, *Phys E: Low-dimens Syst Nanostruct*, 114 (2019) 113608.
15 Weman H, Sirigu L, Karlsson K F, Leifer K, Rudra A & Kapon E, *Appl Phys Lett*, 81 (2002) 2839.
16 Ulhaq A, Ates S, Weiler S, Ulrich S M, Reitzenstein S, Löffler A, Höfling S, Worschech L, Forchel A & Michler P, *Phys Rev B*, 82 (2010) 045307.
17 Nguyen C V, Hieu N N, Poklonski N A, Ilyasov V V, Dinh L, Phong T C, Tung L V & Phuc H V, Phys Rev B, 96 (2017) 125411.
18 Bhat J S, Nesargi R A & Mulimani B G, Phys Rev B, 73 (2006) 235351.
19 Tanatar B & Singh M, *Phys Rev B*, 42 (1990) 3077.
20 Phuc H V, Thao Ng T T, Dinh L & Phong T C, *J Phys Chem Solids*, 75 (2014) 300.
21 Kaasbjerg K, Thygesen K S & Jacobsen K W, *Phys Rev B*, 85 (2012) 165440.
22 Zhang S B & Zhou J, *Phys Rev B*, 101 (2020) 085202.
23 Suzuura H & Ando T, *Phys Rev B*, 65 (2002) 235412.
24 Reinen H A J M, Berendschot T T J M, Kappert R J H & Bluyssen H J A, *Solid State Commun*, 65 (1988) 1495.
25 Phong T C, Phuong L T T, Hien N D & Lam V T, *Phys E: Low-dimens Syst Nanostruct*, 71 (2015) 79.
26 Phuc H V, Hue L T M, Dinh L & Phong T C, *Superlatt Microstruct*, 60 (2013) 508.
27 Meyer H J G, *Phys Rev*, 112 (1958) 298.
28 Vasilopoulos P, *Phys Rev B*, 33 (1986) 8587.
29 Chaubey M P & Vliet C M V, *Phys Rev B*, 33 (1986) 5617.
30 Furno E, Bertazzi F, Goano M, Ghione G & Bellotti E, *Solid State Electron*, 52 (2008) 1796.
31 Makino T, Segawa Y, Tsukazaki A, Ohtomo A & Kawasaki M, *Appl Phys Lett*, 87 (2005) 022101.
32 Baer W S, *Phys Rev*, 154 (1967) 785.
33 Dinh H B, Thu P L T & Cong T, *J Appl Phys*, 123 (2018) 94303.
34 Yang C H, Peeters F M & Xu W, *Phys Rev B*, 82 (2010) 205428.